Available online at www.sciencedirect.com
ScienceDirect
Journal of Environmental Sciences 20(2008) 632–640
JOURNAL OF ENVIRONMENTAL SCIENCES
ISSN 1001-0742
CN 11-2629/X
www.jesc.ac.cn

Effect of spectral resolution on the measurement of monoaromatic hydrocarbons by DOAS

PENG Fumin[1,2], XIE Pinhua[1,*], ZHANG Yinghua[1], ZHU Yanwu[1], SI Fuqi[1], LIU Wenqing[1], WANG Junde[3]

1. Key Laboratory of Environmental Optical and Technology, Anhui Institute of Optics and Fine Mechanics, Chinese Academy of Sciences, Hefei 230031, China. E-mail: pengfm@dicp.ac.cn
2. College of Chemistry and Chemical Engineering, Anhui University, Hefei 230039, China
3. Dalian Institute of Chemical Physics, Chinese Academy of Sciences, Dalian 116023, China

Received 29 July 2007; revised 20 September 2007; accepted 8 October 2007

Abstract

The excellent response characteristics and detection sensitivity with much lower operational cost and the capability to discriminate between the isomer of some monoaromatic hydrocarbons (MAHCs) make differential optical absorption spectroscopy (DOAS) a powerful tool to trace concentration variation of MAHCs. But due to the similarity in chemical structure, those MAHCs have the similar overlapped characteristic absorption structures, which make the selection of instrumental parameter critical to the accurate detection of MAHCs. Firstly, the spectral resolution used in DOAS system determines the nonlinear absorption of O_2 and the mass dependence of characteristic absorption structure; thereby it determines the effect of elimination error of O_2 absorption in the atmospheric spectra for the detection of MAHCs. Secondly, spectral resolution determines the differential absorption characteristics of twelve MAHCs representing major constituents in technical solvents used in the automobile industry and the interference of spectral overlapping. Thirdly, the spectral resolution determines the sensitivity, time resolution and linear range. So the spectral resolution range with the best ratio of signal to noise is used to determine the most suitable spectral resolution range, as well as the spectral resolution range that ensure the characteristic absorption structure of MAHCs and the minimization of O_2 absorption interference. Finally, 0.15–0.16 nm (FWHM: full width at half maximum) is assumed to be closest to the optimum spectral resolution and it is confirmed by the results of practical measurement of MAHCs by DOAS.

Key words: differential optical absorption spectroscopy (DOAS); monoaromatic hydrocarbons (MAHCs); spectral resolution; characteristic absorption structure

Introduction

Today, people pay increased attention to monoaromatic hydrocarbons (MAHCs) due to the growing awareness of their carcinogenic and mutagenic effects on living organisms and human health and their key roles in reactions promoting photochemical smog (Volkamer *et al*., 1998; Etzkorn *et al*., 1999; Kourtidis *et al*., 2002). In order to comply with new regulations and scan pollutants in a large area giving instantaneous measurements of background pollution, the selective and continuous measurement techniques for these species in ambient air are needed. Fourier transform spectroscopy has been used to detect hydrocarbons in the infrared spectral region (Sander *et al*., 1992), but continuous refinements may extend the practical use of this method into the ultraviolet region where the absorption cross sections are larger. Long-path DOAS (differential optical absorption spectroscopy) in the ultraviolet region has been shown to be applicable for the subgroup of light aromatic hydrocarbons (Lee *et al*., 2005; Sandroni *et al.*, 1994). In addition, the isomers of xylene and trimethyl-benzene that could not be separated by traditional methods can be identified and quantified individually by DOAS. However, the application of the DOAS technique for this group of compounds is associated with some problems. One of the most important problems is the similarity and overlapping of characteristic absorption structure of different aromatics, which result in not only large quantitative error, but also incorrect identification of different MAHCs. The similar absorption features of light aromatic hydrocarbons in ultraviolet region originate from excitation of the electrons in the unlocalized π bonds in the benzene ring. It makes the selection of detecting conditions of instrument critical to the accuracy of detected results. In addition, MAHCs usually exist in the atmosphere with trace amounts, which make high sensitivity of instrument necessary.

The effect of spectral resolution (Γ_0), indicated as full width at half maximum (FWHM, nm) used in DOAS system on the magnitude of interference of over-

* Corresponding author. E-mail: xiepinhua@gmail.com.

lapped characteristic absorption structures of MAHCs and accurate detection of MAHCs concentrations was studied. Firstly, the relationships among spectral resolution and the mass dependence nonlinear absorption of O_2 was studied. Secondly, differential absorption features of twelve MAHCs between 250–280 nm were examined and the spectral overlapping between them was investigated. The dependence of the magnitude of interference for spectral overlapping between different species on spectral resolution was studied. Thirdly, the relationships among spectral resolutions and the sensitivity, time resolution and linear range for MACHs measurements by DOAS were all determined. All the results were used to determine the most suitable spectral resolution range combined with the spectral resolution range with the best S/N (the ratio of signal to noise).

1 Experimental and analysis

1.1 Basic principle

The analysis of DOAS spectra is based on the Lambert-Beer's law (Platt, 1994), which can be expressed as:

$$I(\lambda) = I_0(\lambda)\exp\left\{\sum_{i=1}^{n}\begin{array}{l}[-\sigma_i(\lambda)N_i - \sigma'(\lambda)N_i - \\ \varepsilon_R(\lambda) - \varepsilon_M(\lambda)]L\end{array}\right\} + B(\lambda)I \quad (1)$$

where, $I(\lambda)$ is the light intensity after passing through the atmosphere; $I_0(\lambda)$ is the intensity of the light source; λ is the wavelength; $\varepsilon_R(\lambda)$ is the Rayleigh-scattering coefficient; $\varepsilon_M(\lambda)$ is the Mie-scattering coefficient; $\sigma_i'(\lambda)$ is the differential absorption cross section of absorber i; $\sigma_i(\lambda)$ is the broadband absorption of absorber i; N_i is the molecule number of absorber i; $B(\lambda)$ is the other noise; L is the total light path length. Numerical filters and special algorithms remove broadband variation of the cross section as well as the wavelength dependency of the measured spectra due to Rayleigh- and Mie-scattering and the lamp. Therefore, molecules that show narrow-band absorption structures can be measured using this method. Thus, we can define a quantity $I_0'(\lambda)$ as the intensity in the absence of differential absorption (Si *et al*., 2006; Xie *et al*.,2004):

$$I(\lambda) = I_0'(\lambda)\exp(-L\sigma'(\lambda)c) \quad (2)$$

Likewise, a differential optical density D' can be defined as:

$$D' = \log(I_0'(\lambda)/I(\lambda)) = L\sum(\sigma_i'(\lambda)c_i) \quad (3)$$

so

$$c_i = \frac{D_i'(\lambda)}{\sigma_i'(\lambda)L} \quad (4)$$

The species concentration can then be calculated according to Eq.(4) with the differential optical density D' and differential absorption cross section of $\sigma_i'(\lambda)$ substituted for the total quantities D and absorption cross section, respectively. So the most important "signal" in the DOAS spectra is the differential optical density D'.

1.2 Experimental setup

DOAS system: a Cassegrain telescope with a high pressure Xenon short-arc lamp (150 W, Osram, Germany) as light source and a main mirror (220 mm diameter and 645 mm focal length); twelve retro reflectors 375 m away were used to reflect the light back into the telescope, where the light was sent to a spectrometer (Acton500, grating: 1800, 1200 and 600 L/mm blazed at 300, 300 and 500 nm, respectively) via a fiber bundle. Then the light was detected by 1024 pixels photo diode array (PDA) (Hoffman Messtechnik GmbH, Germany) kept at –30°C. A UV band-pass was used to reduce the influence of stray light in the spectrograph on the measurements. The data produced by the detector was digitized by a 16-bit analog-to-digital converter (ADC) and then transmitted to the Hoffman controller. After being processed, the signals were transferred to the computer by RS232.

Three different types of spectra were required: an absorption spectrum of the gaseous species, a lamp spectrum without the absorption of the gaseous species and a spectrum of the background light. The DOAS evaluation algorithm is well described in other articles (Platt, 1994), therefore, and will, only be summarized here. It starts with the subtraction of the "electrical" background, i.e., dark current and offset, from the "raw-spectrum". A polynomial is fit to a part of the spectrum and the differential structure is obtained by dividing the spectrum by the polynomial. Calibration spectra are stored together with information of the optical depth (concentration, path length). Each measurement spectrum is then correlated with the calibration spectra according to classical least-squares fit theory, and the corresponding gas concentrations are calculated. The quality of the data can be estimated from the variance and correlations between the calibration and measurement spectra (Xie *et al*., 2004).

1.3 Analysis of characteristic absorption structure of MAHCs

All MAHCs (monoaromatic hydrocarbons) have similar chemical structure (benzene ring), where one or more hydrogen atoms in the benzene ring are substituted (in this aricle MAHCs refer to twelve familiar aromatics in the atmosphere: benzene, toluene, three isomers of xylene, ethyl-benzene, phenol, three isomers of cresol, 1,2,4-trimethyl-benzene, 1,3,5-trimethyl-benzene). The similar absorption features of MAHCs in ultraviolet region (250–280 nm) originate from excitation of the electrons in the unlocalized π bonds in the benzene ring. This band has a characteristic shape with a considerable amount of fine structures due to vibrational transitions. So the difference among the absorption spectra for MAHCs originates only from the effect of substituents the benzene ring and fine structures due to vibrational transitions. However, only the atoms closest to the benzene ring have the major influence on the electron structure of the π bonds. Adding one more alkyl group to the far end of the substituent (i.e., propyl-benzene to form isobutyl-benzene) has virtually no effect at all on the π bonds and, thus, on the spectral signature. This similarity is obviously a disadvantage when

a spectroscopic method is used to identify and quantify the different species. Although the benzene derivatives show spectral similarities, substitution of hydrogen atoms in benzene with smaller alkyl groups (e.g., methyl or ethyl) changes the spectrum primarily in two ways: (1) a smoothing of the fine structure; (2) a dislocation of the absorption maximum, often towards longer wavelengths.

These phenomena are clearly illustrated in Fig.1 (Etzkorn *et al*., 1999; Trost, 1997). Especially, the difference between chemical structures for toluene and ethyl-benzene is the length of the hydrocarbon chain, so the location of absorption maximum is almost unchanged, and only the fine structure becomes smooth. Almost complete overlapping of their characteristic absorption structures makes the interference serious.

As mentioned earlier, the evaluation of DOAS data is based on the curve fitting by means of a non linear least squares fitting algorithm. The overlapping signal band pass filtered measured spectrum is fitted by a linear combination of the band pass filtered absorption spectra of two or more trace gases with the minimized sum of the square of the standard deviation. Some corrections are usually used in the evaluation of DOAS data (Platt, 1994): (1) a polynomial baseline correction. This correction procedure might, however, introduce systematic errors at high absorbance values, especially for poor spectral resolution; (2) wavelength correction procedure. It is normally used in the DOAS application to correct dislocation of the wavelength scale due to thermal effects and mechanical thrusts, and achieve the best match of the absorption features in the measured spectra. The concentration is then evaluated at the position of best correlation. The correlation between the measured spectrum and the reference spectra is repetitively evaluated, as the reference spectra are shifted one step within a small interval around the zero position. The improper selection of initial value of parameter would lead to an inexplicit result or nonconvergent solution. Thus any little error from data (e.g., noise and distortion of baseline) or assumption of initial value would lead to wrong fitting result. The large enough dissimilarity in absorption spectra is critical to the deconvolution of overlapping signal by the least squares fitting algorithm. When the similarity existed among these overlapped absorption structures become large enough, the curve-fitting method would not be used successfully. The accurate detection of trace MAHCs in the atmosphere by DOAS requires not only the high sensitivity, but also the large enough dissimilarity among the absorption features of MAHCs.

2 Results and discussion

2.1 Effect of spectral resolution on the measurement of MAHCs

2.1.1 Effect of spectral resolution on the optical density of MAHCs

To study the effect of spectral resolution on the optical density of toluene, white cell with certain amount of toluene was placed in the light path of DOAS and was detected. Then the differential absorption spectra of single toluene molecule at different Γ_0 were calculated. All the MAHCs were tested in the same way as toluene and the results are shown in Figs.2 and 3.

The band widths of absorption features of MAHCs were normally two or three times narrower than that of SO_2 and O_3, as shown in Fig.2, so their differential cross section $\sigma'(\lambda)$ with some fine structures were more susceptible to Γ_0. For all MAHCs, when Γ_0 was small, the slight increase of Γ_0 would lead to sharp decrease of $\sigma'(\lambda)$; when Γ_0 increased from 0.15 to 0.3 nm, $\sigma'(\lambda)$ of some species such as *o*-xylene, toluene, etc. decreased almost 50%. With the increase of Γ_0, the effect of Γ_0 on $\sigma'(\lambda)$ became weaker. When Γ_0 was larger than 1.5 nm, $\sigma'(\lambda)$ decreased to a level two magnitudes less than that when Γ_0 was small. Then with the increase of Γ_0, $\sigma'(\lambda)$ was almost unchanged. In another hand, for each MAHCs, the effect of Γ_0 on their $\sigma'(\lambda)$ was different from each other. The $\sigma'(\lambda)$ of *o*-xylene and toluene with much narrower band width was the most

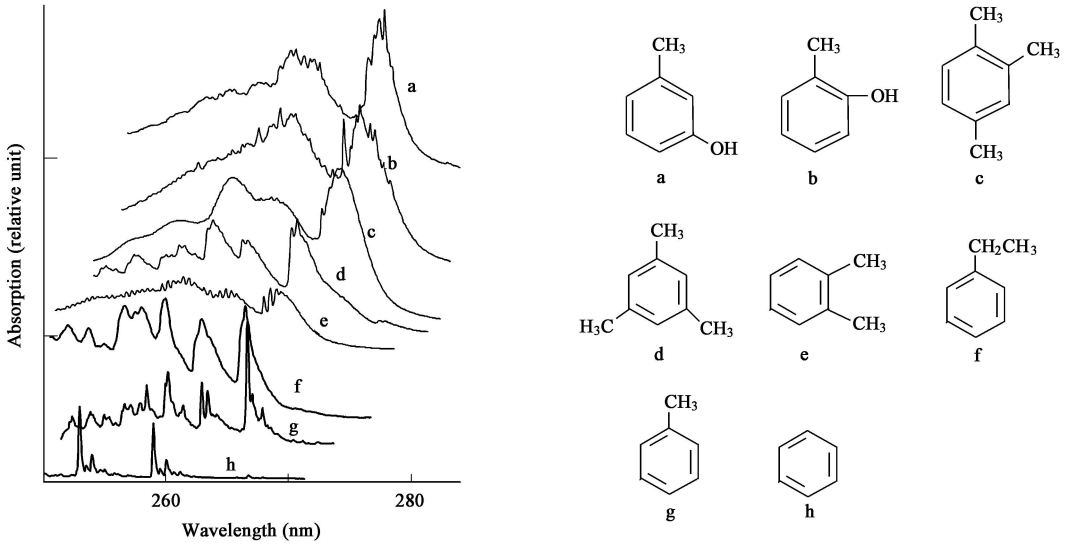

Fig. 1 Absorption cross sections and chemical structures of simple mono-aromatic hydrocarbons. (a) *m*-methyl-phenol; (b) *o*-methyl-phenol; (c) 1,2,4-trimethyl-benzene; (d) 1,3,5-trimethyl-benzene; (e) *o*-xylene; (f) ethyl-benzene; (g) toluene; (h) benzene.

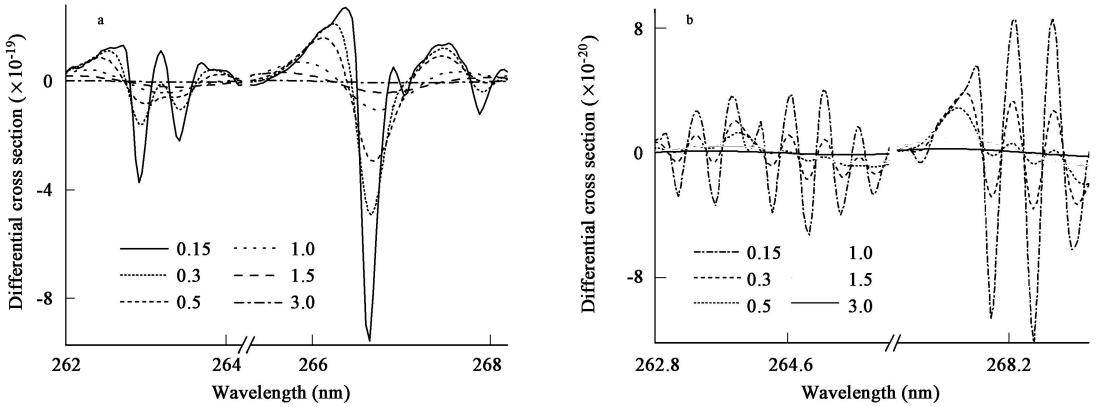

Fig. 2 Differential cross section at different spectral resolutions. (a) toluene; (b) *o*-xylene.

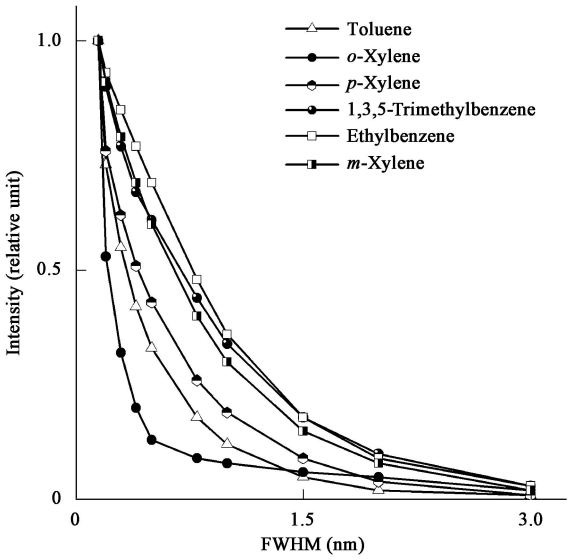

Fig. 3 Absorption optical density of main monoaromatic hydrocarbons (MAHCs) at different spectral resolutions. Full width at half maximum (FWHM): Γ_0 the spectral resolution.

sensitive to Γ_0 and the $\sigma'(\lambda)$ of ethyl-benzene with wider band width was least sensitive to Γ_0. When Γ_0 was small, the largest difference could be seen among the effect of Γ_0 on $\sigma'(\lambda)$ of different species. With the increase of Γ_0, this difference became much less. When $\Gamma_0 > 1.5$ nm, this difference became almost negligible.

In principle, in the DOAS system, the concentration of the absorbing species is determined according to Eq.(4), so the detection limit for a particular substance can be calculated according to:

$$c_{\min} = \frac{D_0}{\sigma'(\lambda, \Gamma_0) \cdot L} \tag{5}$$

So:

$$c_{\min} \propto 1/\sigma'(\lambda) \tag{6}$$

where, D_0 is the minimum detectable optical density; $\sigma'(\lambda, \Gamma_0)$ is the differential absorption cross section of gases at certain wavelength range and Γ_0. It means that when D_0 and L are known, the detection limit would increase as Γ_0 increases. So Γ_0 should be as small as possible for the accurate measurements of MAHCs by DOAS.

2.1.2 Effect of spectral resolution on the linear range of MAHCs

To study the effect of Γ_0 on the linear range of MAHCs, standard gases of toluene with different concentrations were detected at different Γ_0. The selection of standard gas concentrations and cell lengths corresponded to the 1, 5, 50, 100, 150, 200 and 500 ppbv at 700 m light path (standard atmosphere). The detected concentrations of toluene at different Γ_0 were retrieved using reference spectra and the results are shown in Fig.4. In the same way, twelve MAHCs were detected separately.

It is shown that the effect of Γ_0 on the detection error depended on the different species and the concentration. The detected results of toluene and *p*-xylene could be taken as classical samples, as shown in Fig.4. For all the MAHCs, the same characteristic existed as follows: the variation of Γ_0 had very little effect on detection error at low gas concentration. For example, when toluene was about 100 ppbv, the relative error was just several in a thousand. And with the increase of concentration, the effect of Γ_0 on detection error became larger. Especially when Γ_0 was larger than 0.8 nm (Figs.4b and 4d), the relative error increased linearly and the slope increased as Γ_0 increased. For higher concentration conditions, the detected concentration values deviated from standard values at high Γ_0. It can be seen that, as Γ_0 increased, the linear ranges of DOAS for the detection of MAHCs became highly narrower. Assuming 1% was the tolerable upper limit of relative error, the linear range for *p*-xylene at Γ_0 = 0.15 nm was 0–500 ppbv (L = 700 m). When Γ_0 increased from 0.15 nm to 1.5 nm, the linear range of *p*-xylene reduced to about 0–100 ppbv.

On the other hand, even at the same concentration, the effects of Γ_0 on different MAHCs were different. *p*-Xylene and toluene were the most and least sensitive compounds to Γ_0, respectively. For toluene, its linear range was much less sensitive to Γ_0 than *p*-xylene. Besides *p*-xylene, the relative errors of detected *m*-xylene, 1,2,4- and 1,3,5-trimethylbenzene were more sensitive to Γ_0, and the detected concentration values were lees than the actual values. The effect of Γ_0 on the other compounds was

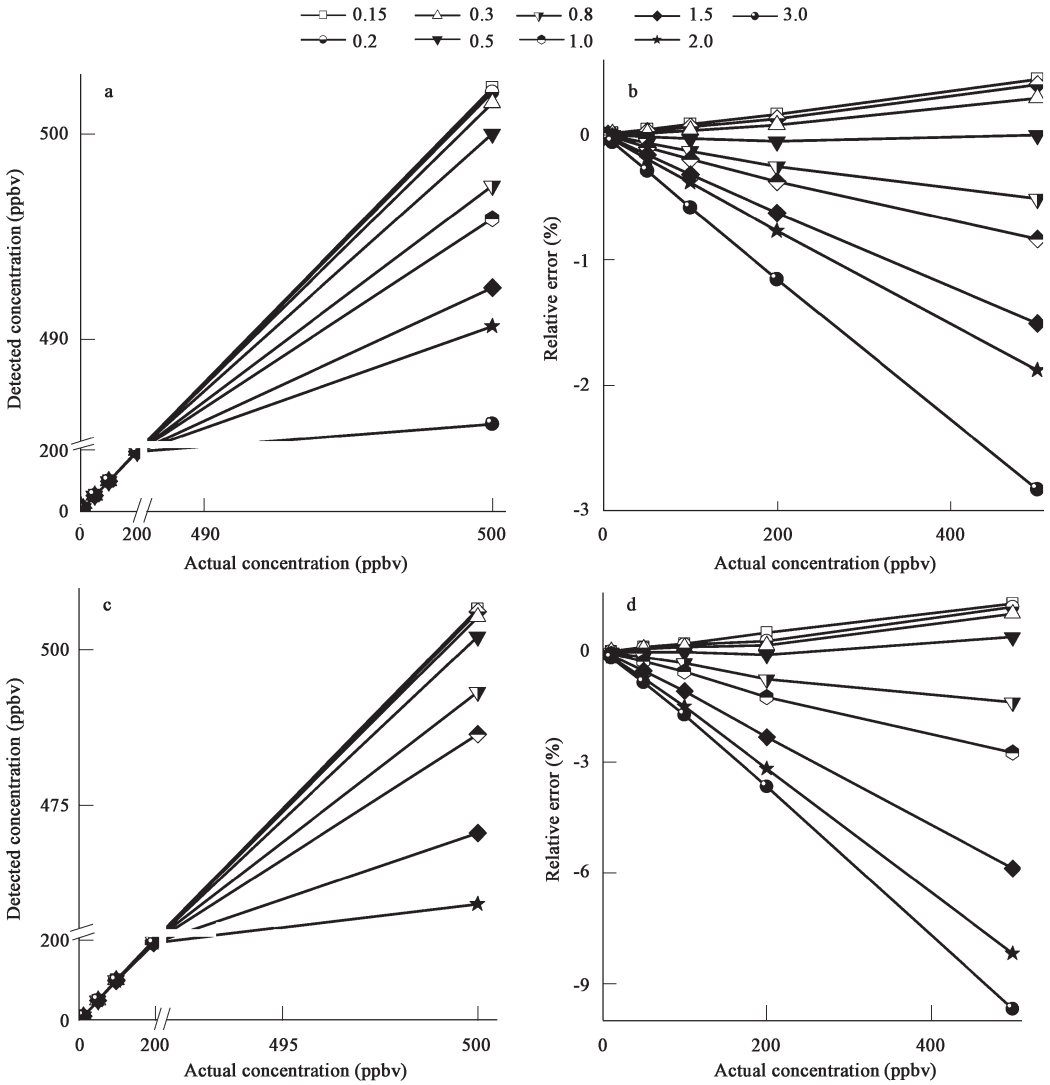

Fig. 4 Effect of spectral resolution on the response intensity of MAHCs with different concentrations. (a) and (b): toulene; (c) and (d): *p*-xylene.

between these two compounds.

2.1.3 Effect of spectral resolution on the characteristic absorption structure

As shown in Fig.5, with the increase of Γ_0, the shape of differential structure and absorption line position of toluene and *o*-xylene changed continuously. In this manner, some spectral features would be lost and, as a consequence, DOAS selectivity would be reduced. The difference existed at low Γ_0 (< 0.15 nm) between the strongest absorption bands of toluene and ethyl-benzene disappeared with the increase of Γ_0. As a result, when they coexisted in the atmosphere, ethyl-benzene could not be identified at high Γ_0 because system could not reveal any specific signature and the retrieved toluene concentration would be higher than the actual value. In the same manner, the difference existed at low Γ_0 between the strongest absorption bands of 1,3,5-trimethylbenzene and *m*-xylene disappeared with the increase of Γ_0 and 1,3,5-trimethylbenzene could not be identified at high Γ_0.

To test the interference effects of spectral overlapping on the DOAS application, the white cell filled with the mixture of twelve MAHCs with known amounts (corresponding to the concentration of 5 ppbv at 700 m light path) was detected by DOAS at different Γ_0. Then the detected concentrations at different Γ_0 were retrieved. As a result, when $\Gamma_0 \leqslant 0.16$ nm, the relative error of ethyl-benzene was less than 1%; when $\Gamma_0 > 0.17$ nm, the relative error increased sharply; when Γ_0 was in the range of 0.19–0.2 nm, ethyl-benzene would not be identified. At the same time, when $\Gamma_0 > 0.2$ nm, the relative error of 1,3,5-trimethylbenzene was more than 1% and when $\Gamma_0 = 0.3$ nm, 1,3,5-trimethylbenzene could not be identified.

2.1.4 Effect of spectral resolution on the nonlinear absorption of O_2

Oxygen (O_2) constituting 21% of the atmosphere by volume shows weak absorption in three Herzberg bands, which covers the ultraviolet region below 300 nm together with the additional diffuse absorption bands due to O_2 isomer (Trankovsky *et al*., 1989). All these bands overlap with the absorption of MAHCs and must always be taken into account as a severe interferent. At low resolving power, the apparent optical density will not increase linearly with the O_2 concentration or the length of light path. The shape of the spectral features will depend on the O_2 column

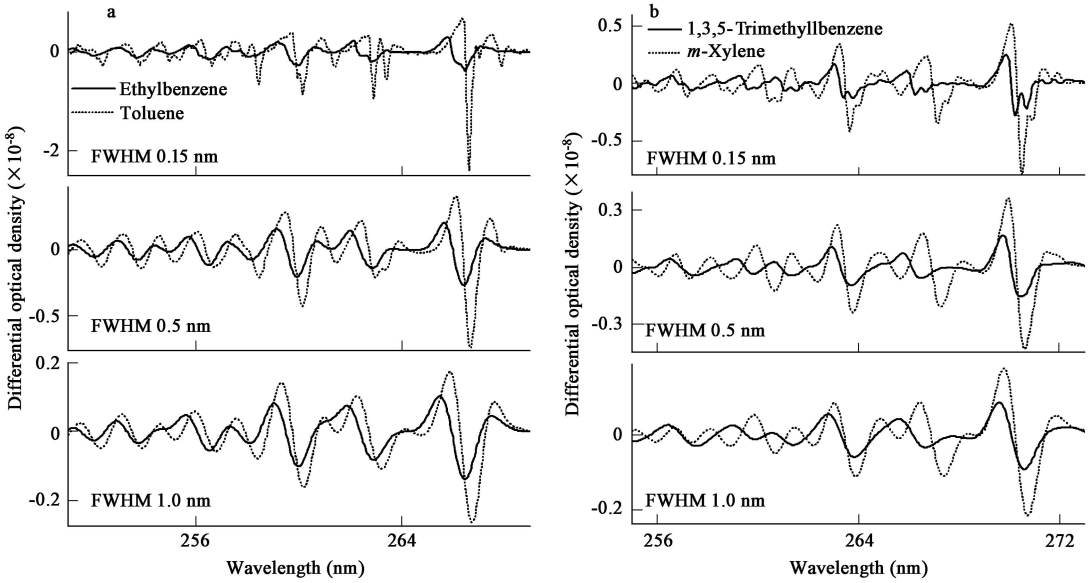

Fig. 5 Effect of spectral resolution on the characteristic absorption structure of MAHCs. (a) toulene and ethylbenzene; (b) 1,3,5-trimethylbenzene and *m*-xylene.

density. To study the influence of Γ_0 on the nonlinearity of O_2 absorption, model calculation based on the Herzberg I band system was carried out to calculate absorption spectra for different column densities of oxygen. The Herzberg I band system contributed the most to O_2 absorption and was more than one order of magnitude stronger than the Herzberg II and Herzberg III systems. Cross sections for ro-vibronic transitions were calculated using the integrated absorption cross sections (Yoshino *et al*., 1995, 1999, 2000). The resulting cross section spectrum was used to calculate absorption spectra for three column densities of oxygen. The column densities were chosen to differ by a constant value and equivalent to a ground level path length in the atmosphere of 400, 800 and 1200 m. Subsequently, these spectra were convoluted with a Gaussian shaped instrument function of 0.05, 0.10, 0.13, 0.15, 0.20 and 0.30 nm (FWHM) to adjust them to a resolution comparable to atmospheric DOAS measurements. As shown in Fig.6, the individual ro-vibronic transitions were not resolved and appeared as Q-branches in the spectrum. When Γ_0 was small (<1 pm), the vertical spacing between three spectra with arithmetical path length should be the same, namely xa=ab=bc, (xa, ab and bc were the vertical spacing between x axis with a, a with b, and b with c, respectively.). However, it could be clearly seen that O_2 absorption apparently deviated from Lambert-Beer's law and the observed optical density of a particular absorption band no longer depended linearly on the column density of oxygen, namely xa≠ab≠bc. The difference between ab and bc depended on the spectral wavelength. Assuming *m*=ab/xa, *n*=bc/xa, *m* and *n* at different wavelengths were different and their trends were different with the increase of Γ_0, as shown in Fig.7; it also indicated that the shape of O_2 absorption depended on the column density of O_2 and this dependence varied with the change of Γ_0 or wavelength range. This nonlinear absorption led to the high residual noise (the difference between the maximum and minimum

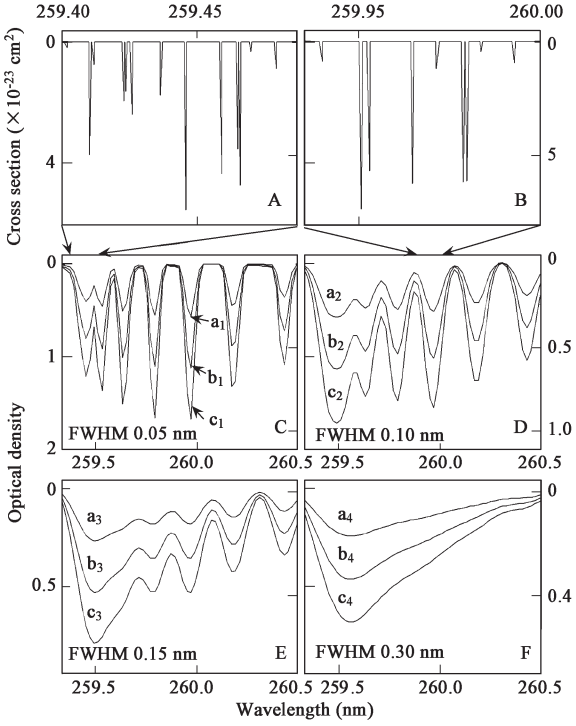

Fig. 6 Absorption spectra of the 5–0 vibronic band of the Herzberg I band system of O_2 at different spectral resolutions. (A) and (B): integrated cross sections of lines of the Herzberg I band system of O_2 at two wavelength ranges; (C), (D), (E), and (F): the Herzberg I band system of O_2 at the spectral resolution of 0.05, 0.10, 0.15, and 0.30 nm. a_i, b_i, c_i: the absorption spectra of O_2 at different spectral resolutions when *L*=400, 800 and 1200 m, respectively.

of the spectrum within the current wavelength range) from several percent (Γ_0=0.05 nm) to several in a thousand (Γ_0=0.5 nm) when 400 and 1200 m absorption spectra were used to correct the absorption features of the 800 m spectrum. However, when 400 and 1200 m absorption spectra were simultaneously used to correct the absorption features of the 800 m spectrum, the nonlinearity of O_2

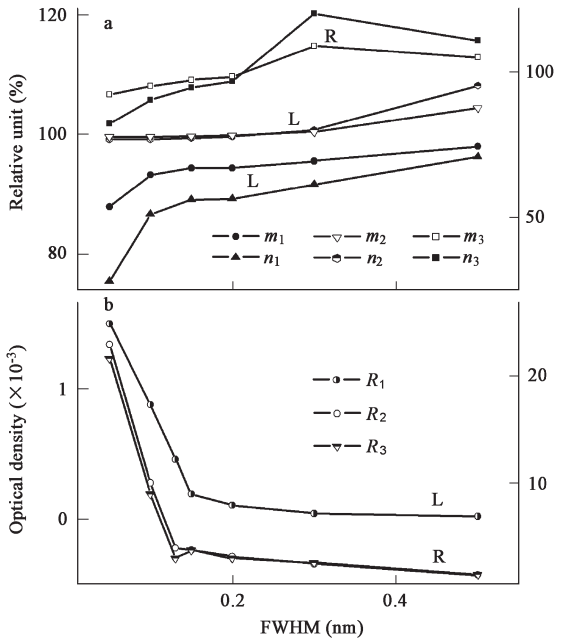

Fig. 7 Effect of spectral resolution on the nonlinearity of O_2 absorption. (a) m_1 and n_1, m_2 and n_2, m_3 and n_3 are obtained at 259.4–259.8, 260.1–260.5, 261.6–262.0 nm, respectively; (b) R_1, R_2 and R_3 are the remained residual after b is fitted by a and c separately and simultaneously. L and R indicate the left and right axes, respectively.

absorption features was not affected greatly by Γ_0, but the residual noise could be reduced to a negligible level.

2.1.5 Effect of spectral resolution on the time resolution

For a given (grating) spectrometer, the light throughput (I_i) varied in proportion to the square of Γ_0, so the detected light intensity (I) became (Platt, 1994):

$$I \approx I_i \propto \Gamma_0^2 \tag{7}$$

For a given species, wavelength, light path and the differential optical density varied in proportion to the concentration, $D' \propto c$. In the case of shot noise limitation, the minimum detectable optical density D_0 in the spectrum was inversely proportional to the square root of I:

$$D_0 \propto I^{-1/2} \tag{8}$$

Thus, to increase S/N and decrease the detection limit, higher light intensity was required. However, with the decrease of Γ_0, especially when Γ_0 was at a low level, I decreased sharply. In general, the light intensity varied in proportion to the exposure time $I \propto t$ (t: exposure time), so with the decrease of Γ_0, t should be increased to recuperate light intensity. As a result, the time resolution of DOAS was decreased, so the time resolution was inversely proportional to the square root of Γ_0.

2.1.6 Determination of optimum resolution

As discussed above, in the MAHCs measurements by DOAS, the accuracy of results was determined by Γ_0, but the effect of Γ_0 on the sensitivity, precise and linear range was contrary with that on the elimination error of O_2 and light intensity. It is necessary to select a most practical Γ_0. The "signal" in the spectrum was the differential optical density D', which would vary in proportional to $\sigma'(\lambda)$ as a function of Γ_0. While $\sigma'(\lambda)$ in principle could be an arbitrary function of Γ_0 (decreasing with the increase of Γ_0), in the example of Fig.8, $\sigma'(\lambda)$ could be simply approximated as a linear function:

$$\sigma'(\Gamma_0) = f(\Gamma_0) \approx \sigma_0'(1-a\Gamma_0) \tag{9}$$

a was a constant

Thus in this case, it could be deduced from Eqs.(6) and (7):

$$D_0 \propto 1/\Gamma_0 \tag{10}$$

The ratio of signal to noise D′/N became:

$$D'/N = \sigma_0'(1-a\Gamma_0)\Gamma_0 \propto \Gamma_0 - a\Gamma_0^2 \tag{11}$$

The optimum D′/N was thus obtained at the resolution:

$$\mathrm{d}(D'/N)/\mathrm{d}\Gamma_0 = 1 - 2a\Gamma_0 = 0 \tag{12}$$

namely

$$\Gamma_{0\mathrm{opt}} = 1/2a \tag{13}$$

As shown in Fig.8, the effect of Γ_0 on σ' varied with different MAHCs, which resulted in different a. Here o-xylene, ethyl-benzene and p-xylene were taken as the examples, because Γ_0 had little, medium and great effect on them, respectively. Based on Fig.8, a could be calculated for o-xylene, ethyl-benzene and p-xylene, separately, and then the corresponding $\Gamma_{0\mathrm{opt}}$ could be determined as 0.13, 0.20 and 0.31 nm, respectively. So the $\Gamma_{0\mathrm{opt}}$ with optimum D′/N varied with different species based on the absorption features. For all the MAHCs, $\Gamma_{0\mathrm{opt}}$ was in the range of $0.13 < \Gamma_{0\mathrm{opt}} < 0.31$ nm.

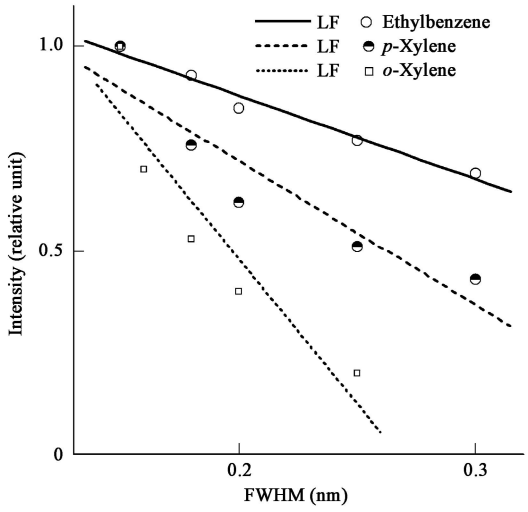

Fig. 8 Relationship between optical density and spectral resolution. LF: linear fitting. In this example, $D(\Gamma_0) \propto \sigma'(\Gamma_0)$, can be simply approximated as a linear function $\sigma'(\Gamma_0)=f(\Gamma_0)\approx\sigma_0'(1\text{-}a\Gamma_0)$, where, a is 3.79, 1.59 and 2.47 for o-xylene, ethylbenzene and p-xylene, respectively.

Obviously, for the determination of Γ_0, the optimum D′/N as well as the loss of selectivity at high Γ_0 and the decrease of linear range should be considered. In addition, when Γ_0<0.15 nm, the residual noise resulted from the elimination error of O_2 absorption increased sharply. All factors considered with respect to the recording of DOAS spectra, 0.15–0.16 nm, therefore, was assumed to be close to an optimum practical resolution, yielding high sensitivity, good selectivity and a reasonable time resolution for the measurements of aromatic compounds by DOAS.

2.2 Practical application

In 2007, long-term continuous MAHCs measurements were carried out by two DOAS systems with the same performance and open light path (L = 713 m) in Hefei City, China. The results from these two systems (A: Γ_0 = 0.15 nm and B: Γ_0 = 0.5 nm) were compared. To eliminate the interference of weather. The data detected under sunny and stable conditions were analyzed and representative results are shown in Fig.9. There is no fixed large emission source near the measurement site, so only toluene, benzene, ethyl-benzene, isomers of xylene and phenol with relatively higher amount in the atmosphere could be detected for a long time by system A and 1,3,5-trimethylbenzene only be detected occasionally. Ethyl-benzene and 1,3,5-trimethylbenzene could not be identified by system B for all the time and toluene was detected with higher concentration by system B than by system A. For other compounds, at low concentrations, the correlation was good between the two systems; at high concentrations, system A showed lower concentrations than system B. Higher Γ_0 was used in system B, so system B showed relatively higher detection limit and could not detect species with lower concentrations, which could be detected by system A. All these results agreed well with the conclusions made above.

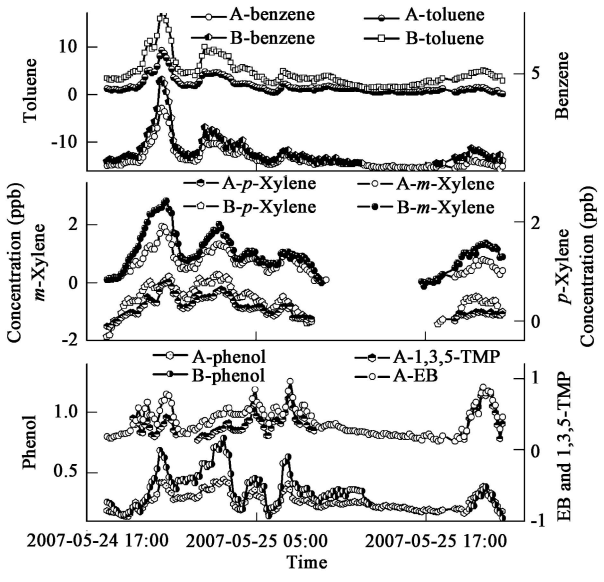

Fig. 9 Time series of benzene, toluene, *p*-xylene, *m*-xylene, phenol, EB (ethyl-benzene) and 1,3,5-TMB (1,3,5-trimethylbenzene) detected by system A and B.

3 Conclusions

The excellent response characteristics and detection sensitivity with much lower operational cost and the capability to discriminate between the isomer of some MAHCs makes DOAS a powerful tool to trace concentration variation of MAHCs. With respect to the recording of DOAS spectra for the accurate measurements of aromatic compounds, the proper selection of spectral resolution can yield high sensitivity, good selectivity, wide linear range and a reasonable time resolution and ensure minimum elimination error for the nonlinear absorption of O_2.

Acknowledgements

This work was supported by the Hi-Tech Research and Development Program (863) of China (No. 2006AA06A303) and the National Natural Science Foundation of China (No. 40675072).

References

Etzkorn T, Klotz B, Sorensen S, Patroescu I, Barnes I, Becker K, Platt U, 1999. Gas-phase absorption cross sections of 24 monocyclic aromatic hydrocarbons in the UV and IR spectral ranges. *Atmospheric Environment*, 33: 525–540.

Kourtidis K, Ziomass I, Zerefos C, Kosmidis E, Symeonidis P, Christophilopoulos E, Karathanassis S, Mploutsos A, 2002. Benzene, toluene, ozone, NO_2 and SO_2 measurement in an urban street canyon in Thessaloniki, Greece. *Atmospheric Environment*, 36: 5355–5364.

Lee Chulkyu, Choi Yeo Jin, Jung Jin Sang, Lee Jeong Soon, Kim Ki Hyun, Kim Young Joon, 2005. Measurement of atmospheric monoaromatic hydrocarbons using differential optical absorption spectroscopy: Comparison with on-line gas chromatography measurements in urban air. *Atmospheric Environment*, 39: 2225–2234.

Platt U, 1994. Differential optical absorption spectroscopy (DOAS). In: Air Monitoring by Spectroscopic Techniques (Sigrist M. W., ed.). New York: Chemical Analysis Series, John Wiley and Sons, Inc. 127: 27–84.

Sander S P, Cageao R P, Friedl R R, 1992. A Compact, high resolution michelson interferometer for atmospheric spectroscopy in the near ultraviolet. In: Optical Methods in Atmospheric Chemistry (Platt U., Schiff H. I., eds.) Berlin, Germany, Proc. SPIE 1715: 15–17.

Sandroni S, Cerutti C, Noriega A, Palmgren F, 1995. Air quality measurements in Brussels (1993–1994). Luxemburg: Published by the European Commission. 37–42.

Si F Q, Liu J G, Xie P H, Zhang Y J, Dou K, Liu W Q, 2006. Determination of size distribution of atmospheric aerosol by DOAS. *Acta Phys Sin*, 55(6): 3165–3169.

Trankovsky E, Ben-Shalom A, Oppenheim U, Devir A, Balfour L, Engel M, 1989. Contribution of oxygen to attenuation in the solar blind UV spectral region. *Applied Optics*, 28: 1588–1591.

Trost B, 1997. UV-absorption cross sections of a series of monocyclic aromatic compounds. *Atmospheric Environment*, 31: 3999–4008.

Volkamer R, Etzkorn T, Geyer A, Platt U, 1998. Correction of the oxygen interference with UV spectroscopic (DOAS) measurement of monocyclic aromatic hydrocarbons in the atmosphere. *Atmospheric Environment*, 32: 3721–3747.

Xie P H, Liu W Q, Fu Q, Wang R B, Liu J G, Wei Q N, 2004. Intercomparison of NOx, SO_2, O_3, and aromatic hydrocarbons measured by a commercial DOAS system and traditional point monitoring techniques. *Advances in Atmospheric Sciences*, 21: 211–219.

Yoshino K, Esmond J R, Murray J E, Parkinson W H, Thorne A P, Learner R C M, Cox G, 1995. Band oscillator strengths of the Herzberg I Bands of O_2. *J Chem Phys*, 103: 1243–1249.

Yoshino K, Esmond J R, Parkinson W H, Thorne A P, Learner R C M, Cox G, 1999. Fourier transform spectroscopy and cross section measurements of the Herzberg II Bands of O_2 at 295 K. *J Chem Phys*, 111: 2960–2967.

Yoshino K, Esmond J R, Parkinson W H, Thorne A P, Learner R C M, Cox G, 2000. Fourier transform spectroscopy and cross section measurements of the Herzberg III Bands of O_2 at 295 K. *J Chem Phys*, 112: 9791–9801.